Available online at www.sciencedirect.com
ScienceDirect
Journal of Solid State Chemistry 181 (2008) 493–498
JOURNAL OF SOLID STATE CHEMISTRY
www.elsevier.com/locate/jssc

Hydrothermal synthesis, structure, and magnetic properties of $Pu(SeO_3)_2$

Travis H. Bray[a], S. Skanthakumar[b], L. Soderholm[b], Richard E. Sykora[c], Richard G. Haire[d], Thomas E. Albrecht-Schmitt[a,*]

[a]Department of Chemistry and Biochemistry and Center for Actinide Science, Auburn University, Auburn, AL 36849, USA
[b]Chemistry Division, Argonne National Laboratory, Argonne, IL 60439, USA
[c]Department of Chemistry, University of South Alabama, Mobile, AL 36688, USA
[d]Chemical Sciences Division, Oak Ridge National Laboratory, Oak Ridge, TN 37831, USA

Received 31 August 2007; received in revised form 18 December 2007; accepted 19 December 2007
Available online 31 December 2007

Abstract

The reaction between PuO_2 and SeO_2 under mild hydrothermal conditions results in the formation of $Pu(SeO_3)_2$ as brick-red prisms. This compound adopts the $Ce(SeO_3)_2$ structure type, and consists of one-dimensional chains of edge-sharing $[PuO_8]$ distorted bicapped trigonal prisms linked by $[SeO_3]$ units into a three-dimensional network. Crystallographic data: $Pu(SeO_3)_2$, monoclinic, space group $P2_1/n$, $a = 6.960(1)$ Å, $b = 10.547(2)$ Å, $c = 7.245(1)$ Å, $\beta = 106.880(9)^\circ$, $V = 508.98(17)$ Å^3, $Z = 4$ ($T = 193$ K), $R(F) = 2.92\%$ for 83 parameters with 1140 reflections with $I > 2\sigma(I)$. Magnetic susceptibility data for $Pu(SeO_3)_2$ are linear from 35 to 320 K and yield an effective moment of $2.71(5)\,\mu_B$ and a Weiss constant of $-500(5)$ K.

Keywords: Plutonium selenite; Plutonium magnetism; Plutonium crystal structure

1. Introduction

The recent resurgence in the structural chemistry of transuranium compounds has brought to light notable differences between the bonding in early actinides and later actinides, as well as discrepancies between these elements and non-radioactive surrogates, e.g. Ce^{4+}. At issue is whether or not transuranium element behavior can be modeled by the lanthanides and early actinides. Notable examples of divergence between the behaviors of these two groups include $PuO_2(IO_3)_2 \cdot H_2O$ [1], whose structure differs substantially from $UO_2(IO_3)_2(H_2O)$ [2], and $[Pu\{5LIO(Me\text{-}3,2\text{-}HOPO)\}_2]$ [3], which is not isostructural with its Ce^{4+} analog [4]. As a part of ongoing investigations concerning the structures and properties of actinide materials containing oxoanions with a non-bonding, but stereochemically active lone-pair of electrons [5], the Pu^{4+} selenite, $Pu(SeO_3)_2$, has been prepared here and its structure compared with that of $Ce(SeO_3)_2$ [6].

Unlike Ce^{4+}, which has a $4f^0$ electron configuration, Pu^{4+} is $5f^4$, and the magnetic susceptibility of $Pu(SeO_3)_2$ is therefore included in this report. The simplest approach appropriate to modeling the magnetic behavior of valence f-states is the Russell–Saunders coupling scheme, which for the f^4 configuration predicts a $^5I_4$ ground level. Although this scheme works well for $4f$ electrons, configuration mixing, intermediate coupling, and bonding considerations all contribute complexity to the accurate representation of $5f$ wavefunctions under a crystal-field potential. In addition, the magnitude of the crystal field may influence the temperature dependence of the susceptibility either through the energy of low-lying excited states or through second-order effects that result in temperature-independent paramagnetism (TIP) [7,8]. There is simply too little known about the magnetic properties of Pu(IV) compounds to begin to untangle these complexities [9]. It is expected that the magnetic behavior of $Pu(SeO_3)_2$ will extend the available examples of the magnetic response in a structurally well-characterized $5f$ compound and, together with a variety of similar results, may provide the experimental

*Corresponding author. Fax: +1 334 844 6959.
E-mail address: albreth@auburn.edu (T.E. Albrecht-Schmitt).

0022-4596/$ - see front matter © 2008 Elsevier Inc. All rights reserved.
doi:10.1016/j.jssc.2007.12.020

basis upon which to extend our theoretical understanding of magnetic coupling.

2. Experimental

2.1. Synthesis

$^{242}PuO_2$ (99.9%, Oak Ridge National Laboratory) and SeO_2 (Alfa-Aesar, 99.4%) were used as received. Reactions were run in PTFE-lined Parr 4749 autoclaves with a 10 mL volume. Distilled and Millipore filtered water with a resistance of 18.2 MΩ cm was used in the reactions. All studies were conducted in a laboratory dedicated to working with transuranium elements, located in a nuclear science facility, and equipped with HEPA-filtered hoods and gloveboxes that are ported directly into the hoods. Counters continually monitor radiation levels in the laboratory. The laboratory is licensed by the state of Alabama (an NRC compliant state) and Auburn University's Radiation Safety Office. All experiments were carried out with approved safety operating procedures. All free-flowing solids are handled in the gloveboxes and solid products are only examined externally after coating with either water or Krytox oil and water.

2.2. $Pu(SeO_3)_2$

PuO_2 (10 mg, 0.036 mmol), SeO_2 (8 mg, 0.072 mmol), and 250 μL of water were loaded in a 10-mL PTFE-lined autoclave. The autoclave was sealed and placed in a preheated furnace for 3 days at 200 °C and then cooled at 9 °C/h to 23 °C. The product consisted of brick-red prisms of $Pu(SeO_3)_2$.

2.3. Crystallographic studies

A single crystal of $Pu(SeO_3)_2$ was mounted on a glass fiber with epoxy, and optically aligned on a Bruker APEX CCD X-ray diffractometer using a digital camera. Intensity measurements were performed using graphite monochromated Mo $K\alpha$ radiation from a sealed tube and monocapillary collimator. SMART (v. 5.624) was used for initial determination of the cell constants and for data collection control. The intensities of reflections of a sphere were collected by a combination of three sets of exposures (frames). Each set had a different ϕ angle for the crystal and each exposure covered 0.3° in ω. A total of 1800 frames were collected with an exposure time per frame of 30 s.

Determination of integrated intensities and global refinement were performed with the Bruker SAINT (v. 6.02) software package using a narrow-frame integration algorithm. A face-indexed numerical absorption correction was initially applied using XPREP [10]. Individual shells of unmerged data were corrected and exported in the same format. These files were subsequently treated with a semi-empirical absorption correction by SADABS [11]. The program suite SHELXTL (v. 6.12) was used for space group determination (XPREP), direct methods structure solution (XS), and least-squares refinement (XL) [10]. The final refinements included anisotropic displacement parameters for all atoms. Selected crystallographic details are given in Table 1. Further details of the crystal structure investigation may be obtained from the Fachinformationzentrum Karlsruhe, D-76344 Eggenstein-Leopoldshafen, Germany (Fax: (+49)7247-808-666; E-mail: crysdata@fiz-karlsruhe.de) on quoting the depository numbers CSD 418050.

Table 1
Crystallographic data for $Pu(SeO_3)_2$

Formula	$Pu(SeO_3)_2$
Formula mass	495.92
Color and habit	Brick-red prism
Crystal system	Monoclinic
Space group	$P2_1/n$ (no. 14)
a (Å)	6.960(1)
b (Å)	10.547(2)
c (Å)	7.245(1)
β (°)	106.880(9)
V (Å^3)	509.0(2)
Z	4
T (K)	193
λ (Å)	0.71073
Maximum 2θ (°)	56.66
ρ_{calcd} (g/cm)	6.472
μ(Mo $K\alpha$) (cm^{-1})	272.04
Number of reflections	4689
Independent reflections	1240
Data/restraints/parameters	1240/0/83
$R(F)$ for $F_o^2 > 2\sigma(F_o^2)$[a]	0.0292
$R_w(F_o^2)$[b]	0.0730

[a] $R(F) = \sum|F_o - F_c| / \sum F_o$.
[b] $R_w(F_o^2) = \left[\sum[w(F_o^2 - F_c^2)^2] / \sum wF_o^4\right]^{1/2}$.

2.4. Magnetic studies

The magnetic susceptibility data were collected on a 18.3 mg powdered sample of $Pu(SeO_3)_2$ using a Quantum Design MPMS 7 SQUID magnetometer. Due to the radiological hazards of ^{242}Pu, the sample was doubly encapsulated in a sealed aluminum holder that contributed significantly (up to 80%) to the measured signals. Empty Al sample holders were measured separately under identical conditions and their magnetic response was subtracted directly from the raw data. Experiments under variable temperatures were carried out between 5 and 320 K under applied fields of 0.5, 2, 5, and 10 kOe. Field measurements, up to 10 kOe, were carried out at 5 and 300 K and revealed a non-linearity to the measured signal as a function of field below about 2000 Oe. The susceptibility was corrected by removing the diamagnetic contribution of the sample from the raw data.

The magnetization of $Pu(SeO_3)_2$ is non-linear with field at fields lower than about 2 kOe. In addition, the measured

susceptibility as a function of temperature (M/H) has a field-dependent component, even at higher fields. Taken together, these observations are consistent with the presence of a ferromagnetic component to the measured magnetic response that has a Curie temperature well above room temperature. Because the ferromagnetic response is so small, this ordered component is assumed to constitute an impurity phase. Assuming for example that the impurity phase was composed of metallic iron, which is ferromagnetic with a Curie temperature of 1043 [12], about 40 ppm in the Pu selenite sample would be sufficient to produce the anomalous field dependence to the data. Following previous precedent for a minor ferromagnetic impurity [13], the magnetization data at two different fields in the linear region, 5000 and 2000 Oe, were subtracted and used to obtain the measured, field-independent, susceptibility used in the analysis.

3. Results and discussion

3.1. Synthesis

The synthesis of $Pu(SeO_3)_2$ proceeded by the dissolution of PuO_2 in selenous acid under hydrothermal conditions, which led to crystallization of $Pu(SeO_3)_2$ that appeared as brick-red prisms.

3.2. Structural features of $Pu(SeO_3)_2$

The structure of $Pu(SeO_3)_2$ is isotypic with that of $Ce(SeO_3)_2$ [6], and consists of one-dimensional chains of edge-sharing PuO_8 units that extend down the a-axis, as shown in Fig. 1. The chains are interconnected by selenite anions to form a dense three-dimensional structure depicted in Fig. 2. There are small channels in the structure that extend down the a-axis to which hold the lone-pair of electrons from the selenite anions. Selected bond distances and angles for the product are given in Table 2. The Pu–O bond distances range from 2.240(5) to 2.495(5) Å. Se–O bonds range from 1.667(5) to 1.735(4) Å for Se(1), and from 1.696(5) to 1.704(5) Å for Se(2) (Table 3).

The geometry of eight-coordinate metal centers in the structure has been the subject of interest for sometime [14]. Four idealized shapes are possible, and include the D_{2d} trigonal dodecahedron found for Pu^{4+} in $Pu(IO_3)_4$ [15], the C_{2v} bicapped trigonal prism, (e.g. for Cf^{3+} in orthorhombic-$CfCl_3$ [16]), the D_{4d} square antiprism observed for Ce^{4+} in $Ce(5LI\text{-}Me\text{-}3,2\text{-}HOPO)_2 \cdot CH_3OH$ [17], and the O_h cubic environment for Pu^{4+} in PuO_2. Raymond and co-workers [17] have developed an algorithm for determining the polyhedron that the eight-coordinate units most closely approximate. We have used this program to evaluate the environment around the Pu centers in $Pu(SeO_3)_2$, and find that they are most closely approximated by a bicapped trigonal prism (C_{2v}, $S = 17.6°$), although its deviation from D_{2d} ($S = 18.8°$) and D_{4d} ($S = 18.7°$) is only slightly more significant.

3.3. Magnetism

Eight-coordinate Pu^{4+} has a $J = 4$ ground manifold. Under an idealized cubic electrostatic field, the manifold is expected to split into a singlet, a doublet, and two triplet states, with the lowest energy state a singlet for all ratios of the fourth to the sixth-order crystal-field parameters [18]. The Pu^{4+} in $Pu(SeO_3)_2$ sits on an eight-coordinate site with C_1 symmetry and as such all symmetry-imposed degeneracies are lifted. The splitting of the resulting nine singlets within the first J manifold is expected to be much larger than kT [19]. Such an electronic structure is expected to produce at lower temperatures only van Vleck TIP, which arises from the mixing by the magnetic field of crystal-field states in different f-ion J manifolds.

The magnetic susceptibility of $Pu(SeO_3)_2$ is shown in Fig. 3. It exhibits a temperature dependence over the entire range of the experiment but there is no evidence of magnetic ordering down to 5 K. Assuming non-interacting, temperature-independent magnetic moments, the magnetic susceptibility can be represented by the Curie–Weiss law:

$$\chi = \frac{C}{T - \theta},$$

where C is the Curie constant related to the effective moment by $\mu_{\text{eff}} = (3kC/N\mu_B^2)^{1/2}$, and θ is the Weiss constant, which is interpreted as a temperature offset to adjust for lower temperature moment correlations [7]. A standard Curie–Weiss plot, shown as an inset in Fig. 3, reveals a linear region to the susceptibility over the temperature range of 35–320 K. The linearity of the data plotted in this manner is consistent with a negligible TIP over this temperature range. A fit to the linear range of the data produces an effective moment of 2.71(5) μ_B and a Weiss constant of −500(5) K.

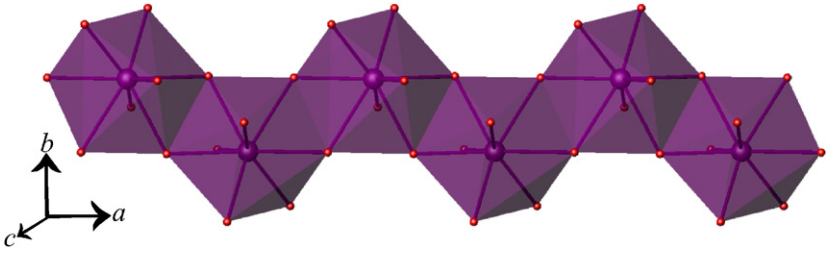

Fig. 1. A view of the one-dimensional chains of edge-sharing PuO_8 dodecahedra that extend down the a-axis in the structure of $Pu(SeO_3)_2$.

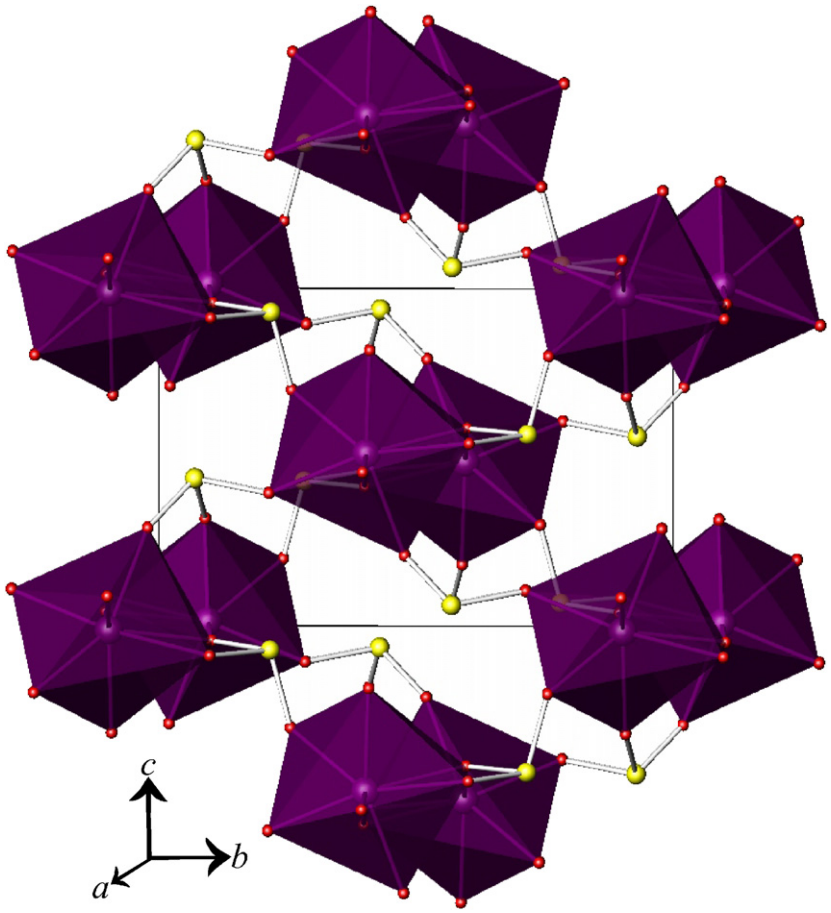

Fig. 2. A depiction of the three-dimensional structure of $Pu(SeO_3)_2$ formed from the interconnection of one-dimensional chains of edge-sharing PuO_8 dodecahedra by selenite anions.

Table 2
Atomic coordinates and equivalent isotopic displacement parameters for $Pu(SeO_3)_2$

Atom (site)	x	y	z	U_{eq} (Å^2)[a]
Pu(1)	0.25883(3)	0.09623(2)	0.01252(3)	0.00790(13)
Se(1)	0.23680(8)	0.28285(6)	0.42993(10)	0.00841(17)
Se(2)	0.27828(9)	−0.06979(6)	−0.43640(10)	0.00948(17)
O(1)	0.1430(6)	0.2422(4)	0.1989(7)	0.0133(9)
O(2)	0.4052(7)	0.4004(4)	0.4126(8)	0.0114(10)
O(3)	0.0711(7)	0.3964(4)	0.4570(7)	0.0116(10)
O(4)	0.1842(6)	0.0213(4)	−0.2898(7)	0.0124(9)
O(5)	0.5261(7)	−0.0904(4)	−0.3172(8)	0.0128(10)
O(6)	0.1928(7)	−0.2142(4)	−0.3938(7)	0.0164(10)

[a] U_{eq} is defined as one-third of the trace of the orthogonalized U_{ij} tensor.

Table 3
Selected bond distances (Å) and angles (°) for $Pu(SeO_3)_2$

Distances (Å)			
Pu(1)–O(1)	2.340(5)	Se(1)–O(1)	1.667(5)
Pu(1)–O(2)	2.356(5)	Se(1)–O(2)	1.713(5)
Pu(1)–O(2)′	2.495(5)	Se(1)–O(3)	1.735(4)
Pu(1)–O(3)	2.324(5)	Se(2)–O(4)	1.698(5)
Pu(1)–O(3)′	2.396(4)	Se(2)–O(5)	1.704(5)
Pu(1)–O(4)	2.243(5)	Se(2)–O(6)	1.696(5)
Pu(1)–O(5)	2.280(5)		
Pu(1)–O(6)	2.240(5)		
Angles (°)			
O(1)–Se(1)–O(2)	100.8(2)	O(4)–Se(2)–O(5)	105.8(2)
O(2)–Se(1)–O(3)	90.0(2)	O(4)–Se(2)–O(6)	100.1(2)
O(1)–Se(1)–O(3)	102.4(2)	O(5)–Se(2)–O(6)	98.6(2)

The effective moment is within error limits of the full free-ion moment of 2.68 μ_B expected for a $^5I_4$ ground level assuming Russell–Saunders coupling. This result is unexpected based on the coordination environment and its splitting of the ground level into singlet states. Even in a cubic crystal field such as that found in PuO_2, in which the metal sits in a cubic site that is also surrounded by eight oxygens, there is an isolated ground state singlet with a triplet state at about 90 meV or higher in energy. As expected, it has no measurable temperature dependence to its susceptibility and an experimentally determined TIP of 536×10^{-6} emu/mol [20,21].

The absence of a TIP term to the susceptibility measured for $Pu(SeO_3)_2$, together with strong evidence that the Pu has a degenerate ground state, raises the question of whether Pu may be trivalent in this material. However, a f^5

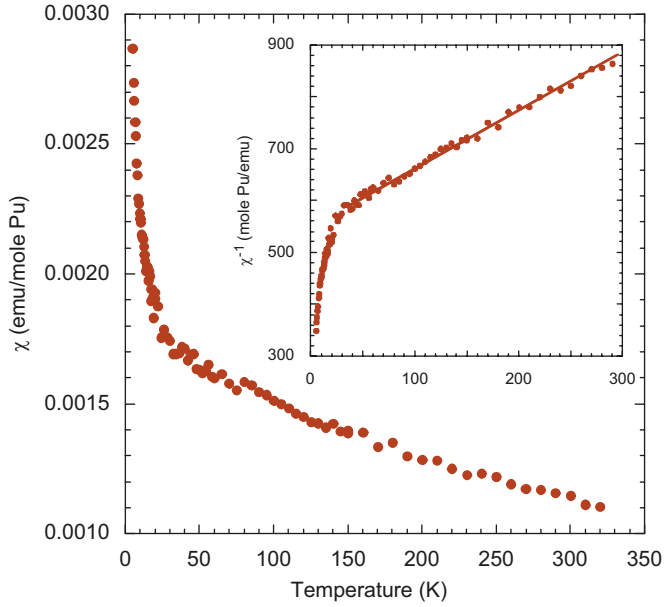

Fig. 3. The magnetic susceptibility of $Pu(SeO_3)_2$ as a function of temperature obtained by subtracting the magnetization measured under an applied field of 2000 Oe from the contribution under a field of 5000 Oe (see text). The temperature dependence at low temperature is not consistent with simple magnetic ordering. The inset shows the same data plotted assuming Curie–Weiss behavior. The solid line, extending over the temperature range of 35–300 K, represents the best fit to the data (see text). The low-temperature deviation from linearity is consistent with the influence of magnetic correlations.

configuration has a free-ion moment of $0.845\,\mu_B$, which is too small to account for the magnetic behavior. In addition, the structural data are consistent with tetravalent Pu, i.e. the bond-valence sum for Pu(1) is 4.45 [22,23].

The inclusion of a Weiss constant in the Curie law is meant to represent the influence at higher temperatures for low-temperature collective or correlated magnetic fluctuations, which are not explicitly included in the simpler model [12]. Within this formalism, a negative value of the Weiss constant could suggest antiferromagnetic interactions. However, the very large value of −500 K found here for the Pu^{4+} selenite would suggest a very strong spin interaction that persists well above room temperature and outside the range of our measurements. The absence of magnetic ordering is not consistent with such a strong coupling. Furthermore, field dependence studies do not support this suggestion. An alternate explanation requires the magnetic moment to change with temperature, a situation that arises when there are low-lying excited crystal-field states that are within kT of the ground state and therefore change population over the temperature range of the experiment. Such changes are known to result in significant deviations from a simple Curie law, which may be incorporated, at least to some extent, into a Weiss constant [8]. Thus, the presence of a large local moment suggests that the C_1 symmetry results in an accidentally degenerate ground state or almost degenerate single states that are thermally populated even at low temperatures.

The susceptibility has been published for two different hydrated sulfates, $Pu(SO_4)_2 \cdot 4H_2O$ and $Rb_4Pu(SO_4)_4 \cdot 2H_2O$ [24,25]. The Pu^{4+} in the hydrated disulfate sits on a low-symmetry site surrounded by eight oxygen atoms, whereas the Pu^{4+} in the hydrated tetrasulfate is coordinated to nine oxygens. Both compounds show deviations from simple Curie Weiss behavior at low temperatures. Fitting the data over 200–335 K results in effective moments of $2.96\,\mu_B$ and Weiss constants of 290 and 830 K, respectively. Similar behavior has been reported for PuF_4, in which the Pu sits in a distorted eight-coordinate site and has a μ_{eff} of $2.90\,\mu_B$ and a θ of 270 K. The latter compound also exhibits a strong TIP contribution below about 150 K. The very large value of the Weiss constants required for fitting the data, coupled with the absence of evidence for magnetic ordering at lower temperatures and unusual temperature dependence, suggests that a simple Curie–Weiss model does not well represent the susceptibility data for these complex chalcogenide–oxide systems.

Data obtained for the Pu monochalcogenides, including PuS, PuSe, and PuTe, have similar temperature dependences to those obtained here for $Pu(SeO_3)_2$ in the sense that they have a sharply rising susceptibility at low temperature but exhibit only TIP above 60 K [26]. These monochalcogonides have the rocksalt structure in which the Pu sits in a six-coordinate, cubic site. Although the oxidation state is unclear, the evidence presented is inconsistent with an intermediate-valent system. The difficulties in fitting the susceptibility data for these monochalcogenides were explained in terms of defect sites that could include charge transfer, a scenario that is ruled out in our case.

The magnetic behavior of $Pu(SeO_3)_2$ is complex and not fully understood. On the one hand, the fit to the data assuming a simple Curie Weiss behavior produces an effective moment in the range expected for an f^4 configuration with no discernable TIP. This would suggest an aggregate of non-interacting spins above about 35 K, consistent with a simple paramagnet. On the other hand, the data fitting requires a Weiss constant of −500 K, a value that suggests very strong magnetic correlations that are not borne out by any evidence of ordering at low temperature. Overall, this system is not well modeled by the Curie–Weiss formalism despite the presence of a well-localized moment that does not order above 5 K. The mechanism by which the Pu acquires such a large ground-state moment in this system is not understood, nor is the apparent large interaction temperature, but these findings are of interest in the broader question of local moment formation, or lack thereof, in simple actinide compounds [27,28].

4. Conclusions

In this report, we have demonstrated that the first Pu^{4+} selenite, $Pu(SeO_3)_2$, is isotypic with its Ce^{4+} analog. The overall structure is described as one-dimensional chains of edge-sharing $[PuO_8]$ units that extend down the *a*-axis and are interconnected by selenite anions to form a dense, three-

dimensional structure. The local geometry around the Pu^{4+} cations, which is crystallographically C_1, is most closely approximated by an idealized C_{2v} bicapped trigonal prism.

The magnetic susceptibility of $Pu(SeO_3)_2$ is complex and not consistent with the predicted Γ_1 singlet, crystal-field ground state but rather by a degenerate ground state. The combined structural and effective moment data are consistent with Pu^{4+}. An intriguing feature of several Pu^{4+} compounds is their rather massive Weiss constants that argue in favor of strong magnetic correlations without any indication of long-range magnetic ordering down to the lowest temperatures studied. This lack of ordering might be ascribed to the long Pu⋯Pu distance of 3.9723(7) Å in $Pu(SeO_3)_2$.

Acknowledgments

This work was supported by the Chemical Sciences, Geosciences and Biosciences Division, Office of Basic Energy Sciences, Office of Science, Heavy Elements Program, US Department of Energy, under grant DE-FG02-01ER15187, and under contracts DE-AC02-06CH11357 at Argonne National Laboratory, and the former contract DE-AC05-00OR22725 with Oak Ridge National Laboratory, managed by UT-Battelle, LLC.

References

[1] W. Runde, A.C. Bean, T.E. Albrecht-Schmitt, B.L. Scott, Chem. Commun. 4 (2003) 478;
A.C. Bean, B.L. Scott, T.E. Albrecht-Schmitt, W. Runde, Inorg. Chem. 42 (2003) 5632.
[2] F. Weigel, L.W.H. Engelhardt, J. Less-Common Met. 91 (1983) 339;
A.C. Bean, S.M. Peper, T.E. Albrecht-Schmitt, Chem. Mater. 13 (2001) 1266.
[3] A.E.V. Gorden, D.K. Shuh, B.E.F. Tiedemann, R.E. Wilson, J. Xu, K.N. Raymond, Chemistry 11 (2005) 2842;
A.E.V. Gorden, J. Xu, K.N. Raymond, Chem. Rev. 103 (2003) 4207.
[4] J. Xu, E. Radkov, M. Ziegler, K.N. Raymond, Inorg. Chem. 39 (2000) 4156.
[5] R.E. Sykora, T.Y. Shvareva, T.E. Albrecht-Schmitt, Structural Chemistry of Inorganic Actinide Compounds, Elsevier Science, 2007.
[6] C. Delage, A. Carpy, A. H'Naïfi, M. Goursolle, Acta Crystallogr. C 42 (1986) 1475.
[7] N.W. Ashcroft, N.D. Mermin, Solid State Physics, Saunders College, Philadelphia, 1976, p. 826.
[8] U. Staub, L. Soderholm, in: K.A. Gschneidner Jr., L. Eyring, M.B. Maple (Eds.), Handbook on the Physics and Chemistry of Rare Earths, Elsevier Science, Amsterdam, 2000, pp. 491–545.
[9] N.M. Edelstein, G.H. Lander, in: L. Morss, N.M. Edelstein, J. Fuger (Eds.), The Chemistry of the Actinide and Transactinide Elements, Springer, Dordrecht, 2006 (Chapter 20).
[10] G.M. Sheldrick, SHELXTL PC, Version 6.12, An Integrated System for Solving, Refining, and Displaying Crystal Structures from Diffraction Data, Siemens Analytical X-ray Instruments, Inc., Madison, WI, 2001.
[11] G.M. Sheldrick, Acta Crystallogr. A 51 (1995) 33.
[12] C. Kittel, Introduction to Solid State Physics, Wiley, New York, 1976, p. 608.
[13] D.L. Gray, L.A. Backus, H.-A.K. Von Nidda, S. Skanthakumar, A. Loidl, L. Soderholm, J.A. Ibers, Inorg. Chem. 46 (2007) 6992.
[14] J.L. Hoard, J.V. Silverton, Inorg. Chem. 2 (1963) 235;
S.J. Lippard, B.J. Russ, Inorg. Chem. 7 (1968) 1686;
M.A. Porai-Koshits, L.A. Aslanov, Russ. J. Struct. Chem. 13 (1974) 244;
E.L. Muetteries, L. Guggenberger, J. Am. Chem. Soc. 96 (1974) 1748.
[15] T.H. Bray, J. Ling, E.-S. Choi, J.S. Brooks, J.V. Beitz, R.E. Sykora, R.G. Haire, D.M. Stanbury, T.E. Albrecht-Schmitt, Inorg. Chem. 46 (2007) 3663.
[16] J.H. Burns, J.R. Peterson, R.D. Baybarz, J. Inorg. Nucl. Chem. 35 (1973) 1171.
[17] J. Xu, E. Radkov, M. Ziegler, K.N. Raymond, Inorg. Chem. 39 (2000) 4156.
[18] K.R. Lea, M.J.M. Leask, W.P. Wolf, J. Phys. Chem. Solids 23 (1962) 1381.
[19] D.J. Newman, B. Ng, J. Phys.: Condens. Matter 1 (1989) 1619.
[20] G. Raphael, R. Lallement, Solid State Commun. 6 (1968) 383.
[21] M. Colarieti-Tosti, O. Eriksson, L. Nordstrom, J. Wills, M.S.S. Brooks, Phys. Rev. B 65 (2002) 195102.
[22] I.D. Brown, D. Altermatt, Acta Crystallogr. B 41 (1985) 244.
[23] N.E. Brese, M. O'Keeffe, Acta Crystallogr. B 47 (1991) 192.
[24] W.B. Lewis, N. Elliott, J. Chem. Phys. 27 (1957) 904.
[25] B. Kanellakopulos, R. Klenze, in: W.T. Carnall, G.R. Choppin (Eds.), Plutonium Chemistry, American Chemical Society, Washington, DC, 1983, pp. 25–40.
[26] G.H. Lander, J. Rebizant, J.C. Spirlet, A. Delapalme, P.J. Brown, O. Vogt, K. Mattenberger, Physica B 146 (1987) 341.
[27] T. Hotta, Reports Prog. Phys. 69 (2006) 2061.
[28] D.G. Karraker, Inorg. Chem. 10 (1971) 1564.